

ChemComm

Chemical Communications

Accepted Manuscript

This article can be cited before page numbers have been issued, to do this please use: Z. Ma, X. Zhang, C. Liu, S. Dong, J. Yang, G. Wu and Z. Xu, *Chem. Commun.*, 2020, DOI: 10.1039/D0CC02555K.



This is an Accepted Manuscript, which has been through the Royal Society of Chemistry peer review process and has been accepted for publication.

Accepted Manuscripts are published online shortly after acceptance, before technical editing, formatting and proof reading. Using this free service, authors can make their results available to the community, in citable form, before we publish the edited article. We will replace this Accepted Manuscript with the edited and formatted Advance Article as soon as it is available.

You can find more information about Accepted Manuscripts in the [Information for Authors](#).

Please note that technical editing may introduce minor changes to the text and/or graphics, which may alter content. The journal's standard [Terms & Conditions](#) and the [Ethical guidelines](#) still apply. In no event shall the Royal Society of Chemistry be held responsible for any errors or omissions in this Accepted Manuscript or any consequences arising from the use of any information it contains.

COMMUNICATION

Polyamide Nanofilms Synthesized via Controlled Interfacial Polymerization on the “Jelly” SurfaceReceived 00th January 20xx,
Accepted 00th January 20xxZhao-Yu Ma,^a Xi Zhang,^a Chang Liu,^a Shun-Ni Dong,^a Jing Yang^{*a}, Guang-Peng Wu^a
and Zhi-Kang Xu ^{*ab}

DOI: 10.1039/x0xx00000x

A thermal-sensitive “jelly” was used to control the diffusion of diamine monomer for synthesizing polyamide free-standing nanofilms with an adjustable thickness of 5-35 nm. The reduced reaction rate of the interfacial polymerization at the hexane-“jelly” interface made the synthesized nanofilms show high water permeation flux and suitable salt rejection, which also have highly negative surface charges and fairly smooth surfaces.

Interfacial polymerization has been indispensably used for synthesizing polyamide (PA) nanofilms, which have been widely used as the selective layers of membranes in forward osmosis,^{1, 2} reverse osmosis,³⁻⁵ nanofiltration⁶⁻⁸ and other separation processes.^{9, 10} Up to now, the commercialized PA-based membranes show great advantages in the fields of solute concentration,¹¹ seawater desalination,^{12, 13} and sewage treatment.^{14, 15} However, it should be noted that synthesizing PA nanofilms with consistent morphologies and adjustable performances is still a tough task. One of the main reasons is the challenge to control the diffusion of monomers and to capture the dynamics of the rapid polymerization occurring at the immiscible organic-aqueous interface.¹⁶

In the cases of nanofiltration, PA nanofilms are commonly synthesized by the interfacial polymerization of diamine and trimesoyl chloride (TMC) at the organic-aqueous interface. The synthesis process is composed of diffusion of diamine monomer (piperazine, in the most case), polycondensation at the interface, and termination of the interfacial polymerization.³ It is obvious that controlling the reaction dynamics is the key issue to tune the structures and the desalination properties of the PA nanofilms. In recent years, several methods have been reported to remarkably improve the separation performance of PA nanofilms, which include

the applications of sacrificial layers from cadmium hydroxide nanostrands,¹⁷ the addition of water-soluble polymer in the aqueous solution,¹⁸ and the usage of nanostructured interlayers from carbon nanotubes¹⁹ and cellulose nanocrystals²⁰ as well as mussel-inspired coatings.²¹ PA films, thicker than 100 nm in most of the cases and thus without desalination properties, were synthesized on the hydrogel surfaces of poly(2-hydroxyethyl methacrylate) and/or poly(acrylamide), which were facile to modify the surfaces of (or encapsulate) hydrogels as suggested by Ding *et al.*²² The original intention of all these methods is controlling the release of diamine monomer for the interfacial polymerization. However, it is still a great challenge to deepen the understanding of the interfacial polymerization by controlling the diamine monomer release, because the porous substrates being used as the storage matrices of the monomers limit the direct characterization of diffusion process.²³ On the other hand, interfacial polymerization at hexane-water interface is too quick to control and to evaluate the diffusion of diamine monomers.²⁴

Herein, we present a new method to effectively control the diffusion of piperazine for synthesizing PA free standing nanofilms. Inspired by jelly, agar hydrogel, a typical thermal-sensitive physical gel, was used as the storage matrix of piperazine.²⁵ Self-standing PA nanofilms have been conveniently synthesized by the interfacial polymerization of TMC and piperazine at the hexane-“jelly” interface combining with the sol-gel and gel-sol conversions. Besides, the diffusion of piperazine can be controlled by means of the non-flowability of “jelly”, which has been demonstrated by NMR. Furthermore, for the first time, the apparent activation energies have been measured, which are indispensable for deepening the understanding of the interfacial polymerization. The PA nanofilms synthesized in this way show reduced thickness, smooth surface, and improved water permeability.

Fig. 1 illustrates the fabrication process of the free-standing PA nanofilms (See detailed experiments in ESI[†]). Firstly, the feasibility is verified for the formation and transformation of agar hydrogel with different concentrations of piperazine. The results show that the addition of piperazine does not affect

^a MOE Key Laboratory of Macromolecular Synthesis and Functionalization, Key Laboratory of Adsorption and Separation Materials & Technologies of Zhejiang Province, Department of Polymer Science & Engineering, Zhejiang University, Hangzhou 310027, China. E-mail: xuzk@zju.edu.cn, jing_yang@zju.edu.cn

^b College of Chemical and Biochemical Engineering, Zhejiang University, Hangzhou 310027, China.

[†] Electronic Supplementary Information (ESI) available. See DOI: 10.1039/x0xx00000x

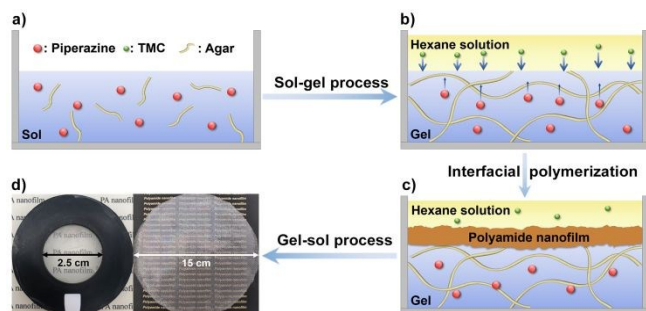


Fig. 1 Schematic illustration for using “jelly” (thermal-sensitive agar hydro-gel) as the storage matrix of piperazine to synthesize PA nanofilms.

the sol-gel process of “jelly”. The concentration of piperazine can be adjusted in a wide range from 0.05 g/L to 10.0 g/L (Fig. S1, ESI[†]), which is suitable for the interfacial polymerization. Typically, a certain amount of agar and piperazine were dissolved in water at 90 °C to form a sol (Fig. 1a). It became like a “jelly” after cooling to room temperature. Then, the hexane solution of TMC was added and the interfacial polymerization was carried out (Fig. 1b, 1c). After that, the “jelly” was heated to 90 °C to melt after removing the residual TMC solution on it. A free-standing PA nanofilm was then obtained after repeated washing with ultrapure water at 90 °C. The PA nanofilm can be easily transferred to different substrates for characterization and performance measurement (Fig. 1d).

We suggest that the non-fluidity nature of “jelly” can slow down the monomer diffusion of piperazine for the interfacial polymerization. However, attempts to dynamically measure the synthesized nanofilms are difficult because they show very slight weight and thin thickness. Thus, a monofunctional benzoyl chloride was used to substitute TMC in the interfacial reaction to demonstrate the role of “jelly” (Fig. 2a, 2c). From the comparison of Fig. 2b and 2d with the standard spectra (Fig. S2, ESI[†]), it can be seen that only the characteristic peak of 1,4-dibenzoylpiperazine (green diamond mark in Fig. 2) is presented in the chloroform-d solution after 5 minutes of reaction in both the aqueous solution and the gel system due to the relatively excess of benzoyl chloride in the organic phase. Thus, the mass of the produced substance can be quantitatively determined by comparing the ratio of the characteristic peak area between products and the internal standard substance (red round mark) under different reaction conditions.²⁶ The quantitative ¹H NMR spectra demonstrate a less production of amides by using the “jelly” matrix under the same conditions. In detail, the diamide produced by the interfacial synthesis using “jelly” is reduced by 10% compared with the original water system according to the quantitative calculation (See detailed experiments in ESI[†]). We propose that the “jelly” could also significantly slow down the interfacial polymerization process by controlling the release of diamine monomer because TMC has lower activity than benzoyl chloride. It is worth noting that the thickness and roughness of the free-standing PA nanofilms are able to be effectively reduced by using “jelly” to store the diamine monomer. On the one hand, the “jelly” surface is quite smooth, which provides an ideal interface for the interfacial

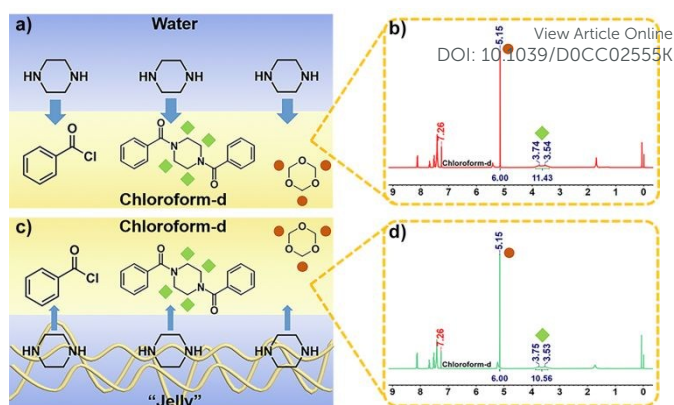


Fig. 2 Schematic illustration showing the diffusion process of piperazine in quantitative NMR experiments. Piperazine was stored in a) water and c) “jelly” respectively, reacting with benzoyl chloride in chloroform-d to form amide as shown. b) and d) ¹H NMR spectra of the products in chloroform-d from a) and c), respectively. A precisely quantified 1,3,5-trioxane was added into the nuclear magnetic tube as the internal standard (chemical shift: ca. 5.1 ppm).

polymerization.^{27, 28} The fluctuant situations of the interfaces are quite different when n-hexane solution was added to the water surface and the “jelly” surface, respectively (Fig. S3, ESI[†]). There are less ripples on the solid-like “jelly” surface compared with the water surface in the case of continuously dropping of n-hexane solution at a fixed height (Movie S1, ESI[†]). The additional fluctuations of the interface during the reaction could result in rougher PA nanofilms. Unlike the free hexane-water interface, the hexane-“jelly” interface is steadier under external disturbance (Movie S2, ESI[†]), which means that it is facile for us to synthesize large-area PA nanofilms with uniform thickness and roughness. PA nanofilms with a diameter of 15 cm have been successfully synthesized and loaded on a rounded metal mesh (Fig. S4, ESI[†]). On the other hand, the thermosensitive nature of “jelly” allows us to easily explore the effects of temperature on the synthesis of PA nanofilms. The gelation of agar is caused by the existence of hydrogen bonds, and all factors that can destroy the hydrogen bonds can cause the destruction of gelation. Among them, temperature is one of the most important factors. The hydrogen bond network tends to gradually collapse with the increasing temperature, which means that the molecules originally bound in the gel will have greater activity in higher temperature.

We can even estimate the apparent activation energy of the interfacial polymerization after the correspondence between the reaction temperature and the thickness of PA nanofilms was obtained, which are indispensable for deepening the understanding of the whole process of interfacial polymerization. The reaction process and the resulting PA nanofilms were simplified, and then we successfully obtained the activation energy (See detailed derivation in ESI[†]). $E_a \approx 34$ kJ·mol⁻¹ is obtained from the slope of the fitted line (Fig. 3a). Similar result ($E_a \approx 32$ kJ·mol⁻¹) is also drawn from the changes of the surface roughness of the PA nanofilms synthesized at different temperatures (Fig. 3b). These activation energies indicate that the reaction process is a fairly fast transition between two immiscible phases although the gel is already applied for reducing the diffusion of piperazine. When the two phases containing two reactive monomers respectively are in

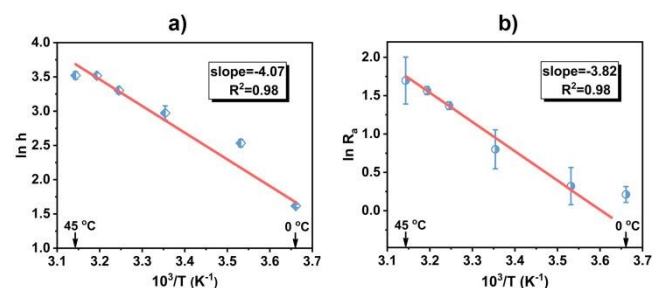


Fig. 3 Estimation of the apparent activation energies for the interfacial polymerization according to a) the thickness and b) the surface roughness of the free-standing PA nanofilms.

contact, the diffusion of diamine occurs immediately, along with the rapid reaction between TMC and piperazine, leading to an incipient PA nanofilm within few seconds.²⁹ It is also the reason why the traditional interfacial polymerization process is difficult to control, and the surface of the PA nanofilms fabricated by ordinary technique are usually crinkly.

Using the “jelly” surface to suppress the monomer diffusion endows the prepared PA nanofilms unique properties as well. The thickness of the PA nanofilms is obviously reduced by lowering the reaction temperature from 45 °C to 0 °C (Fig. S5 and S6, ESI†).³⁰ Moreover, the surface roughness has the same trend and remains below 10 nm (Fig. S7, ESI†), which may help to reduce the membrane fouling in practical applications.³¹ We can even synthesize intact PA nanofilms with a thickness down to 5 nm, which is far thinner than most literature reports.³² Besides, the surface potential of the PA nanofilms (-80 mV at pH=7) is much lower than that reported in many other literatures for PA-based membranes prepared using different method (Fig. S9, Table S2, ESI†).^{31, 33, 38} Thinner thickness and lower surface charge mean the PA nanofilms have potential to increase water permeability and salt rejection simultaneously in a pressure-driven nanofiltration process.

In practical applications, the PA nanofilm often acts as a selective layer supported by a porous substrate to form composite membrane. In our cases, the free-standing PA nanofilms are facilely composited with polyether sulfone substrate by vacuum filtration after the gel was heated to sol. The nanofiltration performance can be tuned by controlling the synthesis of PA nanofilms. Firstly, the content of piperazine in “jelly” have a large impact. In general, water permeability declines with the increases of piperazine concentration in “jelly” (Fig. 4a). When the concentration of piperazine is less than 0.1 g/L, the PA nanofilms are too thin to hold the pressurized conditions, which is reflected in the sharp drop in salt rejection and the pore profiles of the polyether sulfone substrate beneath the nanofilms shown in the SEM images (Fig. S10 and S11, ESI†). As the concentration of piperazine increases, the synthesized PA nanofilms become thicker and the surface generates some typical nodal protrusions. However, when come to the concentration of TMC, it only slightly affects the separation performance of the PA nanofilms (Fig. S12, ESI†).

Another important factor affecting the nanofiltration performance is the temperature at which the PA nanofilms been synthesized. The water permeability ranges from 15 to

34 $\text{Lm}^{-2}\text{h}^{-1}\text{bar}^{-1}$ when the reaction temperature changes from 45 °C to 0 °C (Fig. 4b). The same trend is also found in nanofilms synthesized at free hexane-“jelly” interface (Fig. S13, ESI†). This phenomenon is mainly due to the suppressed diffusivity of piperazine at lower temperature and the resulting thinner PA nanofilms.^{5, 29} It is worth noting that although the thickness of the PA nanofilm is sub-10 nm, it still retains a high rejection to Na_2SO_4 . Also, with the increasing reaction temperature, the surface of the PA nanofilms remain flat (Fig. S14, ESI†).

The PA nanofilms synthesized on the “jelly” surface show the salt rejection sequence as: Na_2SO_4 (97.7%) > MgSO_4 (90.5%) > NaCl (15.1%) > MgCl_2 (11.1%). This phenomenon result from the Donnan effect and the steric effect.³⁴ Taking the hydrolysis of TMC groups promoting the formation of negatively charged surface into consideration, controlling the diffusion of piperazine makes a smaller amount of piperazine diffusing into the organic phase, which is immediately reacted by abundant TMC once it entered, leading to more negatively surface charge of PA nanofilms. When applying the PA nanofilms to nanofiltration process, the lower surface charge allows it exhibit superior divalent anion rejection (~98%), while maintaining good permeability to monovalent anions (Fig. 4c). With the help of reduced thickness and lower surface charge, PA nanofilms prepared by our method show outstanding nanofiltration performance (Fig. 4d).^{6-8, 18-21, 31, 35-46}

In summary, we have demonstrated a novel method to synthesize PA nanofilms via interfacial polymerizing piperazine and trimesoyl chloride at the hexane-“jelly” interface. Intact PA nanofilms have been fabricated with smooth surface and quite thin thickness with the help of a more stable interface

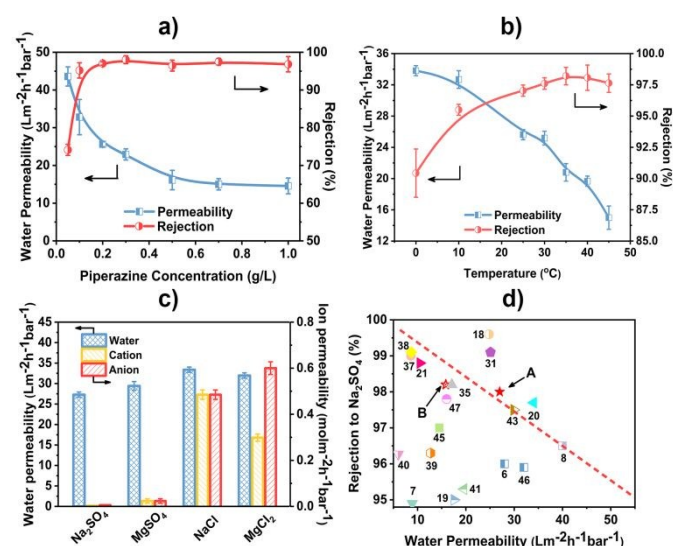


Fig. 4 Nanofiltration properties of the PA nanofilms. a) Water permeability and salt rejection to Na_2SO_4 of the PA nanofilms synthesized using different concentrations of piperazine in “jelly”. The TMC in hexane is 1.0 g/L. (Na_2SO_4 concentration: 1000 ppm; applied pressure: 4 bar) b) Effect of the reaction temperature on the permselectivity of the PA nanofilms. (piperazine/TMC = 0.2/0.7 g/L; Na_2SO_4 concentration: 1000 ppm; applied pressure: 4 bar) c) Mono/divalent ion selectivity for four salts of the PA nanofilms. (salt concentration: 1000 ppm; applied pressure: 4 bar) d) Nanofiltration performance of some state-of-the-art composite membranes reported in literatures. A: PA nanofilm synthesized at hexane-“jelly” interface, B: PA nanofilm synthesized at hexane-water interface (piperazine/TMC = 0.2/0.7 g/L).

provided by the “jelly”. The apparent activation energies of the interfacial polymerization have been estimated for the first time by controlling the reaction temperature. The desalination properties of the PA nanofilms can be conveniently tuned by adjusting the concentration of piperazine and the temperature of the interfacial polymerization. The synthesized PA nanofilms show remarkably high water permeance while preserving salt rejection in practical nanofiltration process. This new synthetic system is expected to be a simple but efficient tool to help to deepen the understanding of interfacial polymerization between polyamines and poly(acid chloride)s, and other interfacial reactions.

This work is financially supported by the National Natural Science Foundation of China (Grant No. 21534009).

Conflicts of interest

There are no conflicts to declare.

Notes and references

- N. Y. Yip, A. Tiraferri, W. A. Phillip, J. D. Schiffman and M. Elimelech, *Environ. Sci. Technol.*, 2010, **44**, 3812-3818.
- J. Wei, C. Qiu, C. Y. Tang, R. Wang and A. G. Fane, *J. Membr. Sci.*, 2011, **372**, 292-302.
- Z. Jiang, S. Karan and A. G. Livingston, *Adv. Mater.*, 2018, **30**, e1705973.
- C. Liu, C. Wang, Y. Guo, J. Zhang, Y. Cao, H. Liu, Z. Hu and C. Zhang, *J. Mater. Chem. A*, 2019, **7**, 6695-6707.
- S.-J. Park, W. Choi, S.-E. Nam, S. Hong, J. S. Lee and J.-H. Lee, *J. Membr. Sci.*, 2017, **526**, 52-59.
- Z. Zhai, C. Jiang, N. Zhao, W. Dong, H. Lan, M. Wang and Q. J. Niu, *J. Mater. Chem. A*, 2018, **6**, 21207-21215.
- Y. He, J. Liu, G. Han and T.-S. Chung, *J. Membr. Sci.*, 2018, **555**, 299-306.
- S. Gao, Y. Zhu, Y. Gong, Z. Wang, W. Fang and J. Jin, *ACS Nano*, 2019, **13**, 5278-5290.
- S. Zhang, P. Wang, X. Fu and T. S. Chung, *Water Res.*, 2014, **52**, 112-121.
- S. Li, Z. Wang, C. Zhang, M. Wang, F. Yuan, J. Wang and S. Wang, *J. Membr. Sci.*, 2013, **436**, 121-131.
- M. Li, X. Wang, C. J. Porter, W. Cheng, X. Zhang, L. Wang and M. Elimelech, *Environ. Sci. Technol.*, 2019, **53**, 3078-3086.
- A. F. Ismail, M. Padaki, N. Hilal, T. Matsuura and W. J. Lau, *Desalination*, 2015, **356**, 140-148.
- Y. Hu, K. Lu, F. Yan, Y. Shi, P. Yu, S. Yu, S. Li and C. Gao, *J. Membr. Sci.*, 2016, **501**, 209-219.
- K. Luttmiah, A. R. Verliefde, K. Roest, L. C. Rietveld and E. R. Cornelissen, *Water Res.*, 2014, **58**, 179-197.
- S. Kim, K. H. Chu, Y. A. J. Al-Hamadani, C. M. Park, M. Jang, D.-H. Kim, M. Yu, J. Heo and Y. Yoon, *Chem. Eng. J.*, 2018, **335**, 896-914.
- H. B. Park, J. Kamcev, L. M. Robeson, M. Elimelech and B. D. Freeman, *Science*, 2017, **356**, eaab0530.
- S. Karan, Z. Jiang and A. G. Livingston, *Science*, 2015, **348**, 1347-1351.
- Z. Tan, S. Chen, X. Peng, L. Zhang and C. Gao, *Science*, 2018, **360**, 518-521.
- M.-B. Wu, Y. Lv, H.-C. Yang, L.-F. Liu, X. Zhang and Z.-K. Xu, *J. Membr. Sci.*, 2016, **515**, 238-244.
- J.-J. Wang, H.-C. Yang, M.-B. Wu, X. Zhang and Z.-K. Xu, *J. Mater. Chem. A*, 2017, **5**, 16289-16295. DOI: 10.1039/D0CC02555K
- X. Zhang, Y. Lv, H. C. Yang, Y. Du and Z. K. Xu, *ACS Appl. Mater. Interfaces*, 2016, **8**, 32512-32519.
- M. Wang, C. M. Stafford, L. M. Cox, A. K. Blevins, M. Aghajani, J. P. Killgore and Y. Ding, *Macromol. Chem. Phys.*, 2019, **220**, 1900100.
- N. Misdan, W. J. Lau, A. F. Ismail, T. Matsuura and D. Rana, *Desalination*, 2014, **344**, 198-205.
- A. Nowbahar, V. Mansard, J. M. Mecca, M. Paul, T. Arrowood and T. M. Squires, *J. Am. Chem. Soc.*, 2018, **140**, 3173-3176.
- M. L. Oyen, *Int. Mater. Rev.*, 2013, **59**, 44-59.
- G. F. Pauli, T. Godecke, B. U. Jaki and D. C. Lankin, *J. Nat. Prod.*, 2012, **75**, 834-851.
- P. Zhang, F. Zhang, C. Zhao, S. Wang, M. Liu and L. Jiang, *Angew. Chem. Int. Ed. Engl.*, 2016, **55**, 3615-3619.
- Q. Hao, C. Zhao, B. Sun, C. Lu, J. Liu, M. Liu, L. J. Wan and D. Wang, *J. Am. Chem. Soc.*, 2018, **140**, 12152-12158.
- J. Zhu, J. Hou, R. Zhang, S. Yuan, J. Li, M. Tian, P. Wang, Y. Zhang, A. Volodin and B. Van der Bruggen, *J. Mater. Chem. A*, 2018, **6**, 15701-15709.
- B. Khorshidi, T. Thundat, B. A. Fleck and M. Sadrzadeh, *Sci. Rep.*, 2016, **6**, 22069.
- W. Choi, S. Jeon, S. J. Kwon, H. Park, Y.-I. Park, S.-E. Nam, P. S. Lee, J. S. Lee, J. Choi, S. Hong, E. P. Chan and J.-H. Lee, *J. Membr. Sci.*, 2017, **527**, 121-128.
- C. Bellona, J. E. Drewes, P. Xu and G. Amy, *Water Res.*, 2004, **38**, 2795-2809.
- Z. Sun, Q. Wu, C. Ye, W. Wang, L. Zheng, F. Dong, Z. Yi, L. Xue and C. Gao, *Nano Lett.*, 2019, **19**, 2953-2959.
- X. L. Wang, T. Tsuru, S. Nakao and S. Kimura, *J. Membr. Sci.*, 1997, **135**, 19-32.
- F. Yan, H. Chen, Y. Lü, Z. Lü, S. Yu, M. Liu and C. Gao, *J. Membr. Sci.*, 2016, **513**, 108-116.
- S. Liu, C. Wu, W.-S. Hung, X. Lu and K.-R. Lee, *J. Mater. Chem. A*, 2017, **5**, 22988-22996.
- D. Ren, X.-T. Bi, T.-Y. Liu and X. Wang, *J. Mater. Chem. A*, 2019, **7**, 1849-1860.
- B. Yuan, C. Jiang, P. Li, H. Sun, P. Li, T. Yuan, H. Sun and Q. J. Niu, *ACS Appl. Mater. Interfaces*, 2018, **10**, 43057-43067.
- Y.-S. Guo, Y.-F. Mi, F.-Y. Zhao, Y.-L. Ji, Q.-F. An and C.-J. Gao, *Sep. Purif. Technol.*, 2018, **206**, 59-68.
- R. Zhang, S. Yu, W. Shi, W. Wang, X. Wang, Z. Zhang, L. Li, B. Zhang and X. Bao, *J. Membr. Sci.*, 2017, **542**, 68-80.
- Z. Yang, Z. W. Zhou, H. Guo, Z. Yao, X. H. Ma, X. Song, S. P. Feng and C. Y. Tang, *Environ. Sci. Technol.*, 2018, **52**, 9341-9349.
- C. Jiang, L. Tian, Z. Zhai, Y. Shen, W. Dong, M. He, Y. Hou and Q. J. Niu, *J. Membr. Sci.*, 2019, **589**, 117244.
- Y. Ren, J. Zhu, S. Cong, J. Wang, B. Van der Bruggen, J. Liu and Y. Zhang, *J. Membr. Sci.*, 2019, **585**, 19-28.
- Z. Zhang, G. Kang, H. Yu, Y. Jin and Y. Cao, *J. Membr. Sci.*, 2019, **570-571**, 403-409.
- J. Zhu, S. Yuan, A. Uliana, J. Hou, J. Li, X. Li, M. Tian, Y. Chen, A. Volodin and B. Van der Bruggen, *J. Membr. Sci.*, 2018, **554**, 97-108.
- Y. Zhu, W. X. S. Gao, F. Zhang, W. Zhang, Z. Liu and J. Jin, *Small*, 2016, **12**, 5034-5041.
- H. Peng, Q. Tang, S. Tang, J. Gong and Q. Zhao, *J. Membr. Sci.*, 2019, **592**, 117386.